

Infrared Spectroscopy and Raman Spectroscopy Evidences of Silver Replacement into Cu(1) Site in $\text{YBa}_2\text{Cu}_4\text{O}_8$

Yuichi SAWAI, Kozo ISHIZAKI and Yutaka NARUKAWA*

Nagaoka Gijutsu Kagaku Daigaku (Nagaoka University of Technology), Kamitomioka 1603-1, Nagaoka 940-21

*Kobe Steel Co., Ltd., 2-3-1, Shinhaman, Arai-cho, Takasago-shi, Hyogo 676

$\text{YBa}_2\text{Cu}_4\text{O}_8$ の Cu(1) への銀置換に対する赤外吸収スペクトル及びラマンスペクトルによる証拠

沢井裕一・石崎幸三・成川 裕*

長岡技術科学大学, 940-21 新潟県長岡市上富岡町 1603-1

*(株)神戸製鋼所, 676 兵庫県高砂市荒井町新浜 2-3-1

[Received September 13, 1993; Accepted January 27, 1994]

$\text{YBa}_2(\text{Cu}_{1-x}\text{Ag}_x)_4\text{O}_8$ ($x < 0.1$) superconductor was synthesized under high oxygen partial pressures by oxygen hot isostatic press. From Raman scattering spectroscopy, the phonon frequency of O(4)-Cu(1) stretching vibration increased and that of O(1)-Cu(1) vibration decreased by doping silver. Phonon frequency change is due to an increase in the force constant of O(4)-Cu(1) bond and to a decrease in the force constant of O(1)-Cu(1) bond by a silver replacement into the Cu(1) site. Ag-O bondings are detected in the 124 phase by an infrared absorption spectroscopy also. The evidence of silver replacement into Cu(1) site in $\text{YBa}_2\text{Cu}_4\text{O}_8$ was presented for the first time.

Key-words: $\text{YBa}_2\text{Cu}_4\text{O}_8$, O_2 -HIP, IR spectra, Raman spectra, Silver replacement

1. Introduction

Many researchers have sintered $\text{YBa}_2\text{Cu}_3\text{O}_7$ (123 phase) superconductors with an addition of Ag_2O or AgO to improve mechanical and superconducting properties. The reported improvements are; an increase in the critical current density,¹⁾⁻⁴⁾ an increase in the critical temperature,^{2),4),5)} and enhancement in the bulk sinterability.^{2),3),6),7)} Other researchers reported, however, a decrease in the critical temperature³⁾ or no change⁷⁾ by doping silver.

Almost all researchers reported that silver doping caused no distinct microstructural changes of the 123 phase. Doped silver segregates in voids between particles or diffuses to grain boundaries or surfaces of particles.^{3),8)} Lin et al., however, have found that doped silver atoms located at the Cu(1) sites in the 123 phase by the IR absorption method.⁹⁾ Cu(1) is defined in the next chapter. Kolesov et al. have also reported a silver replacement into the Cu(1) site in the 123 phase, and proved it by Raman scattering method.¹⁰⁾ Ren et al.⁴⁾ and Choy et al.¹¹⁾ have reported further the substitution by X-ray diffraction method and lattice parameter measurements. But there has been no work reported on $\text{YBa}_2\text{Cu}_4\text{O}_8$ (124 phase).

We have already reported that the critical temperature, T_c , of the 124 phase increased by AgO doping.⁵⁾ In the present work, a silver replacement into the Cu(1) site in the 124 phase is discussed by IR absorption and Raman scattering methods.

2. Crystal structure and vibration modes of $\text{YBa}_2\text{Cu}_4\text{O}_8$

The 124 structure contains double CuO chains (instead of single in 123 structure), and the arrangement of the oxygen atoms and vacancies in the double CuO chains appears to be completely ordered, as shown in Fig. 1. This is a result of a shift of the second CuO layer with respect to the first one by a half of the b -axis lattice parameter.²⁹⁾ It leads to higher coordination of oxygen in the chains, each oxygen atom has three nearest copper atoms. The higher coordination causes higher stability of the oxygen in the 124 phase (up to 880°C). Top and bottom planes in Fig. 1 are basal conduction planes. Copper atoms on the chains are called Cu(1), and copper atoms on the basal planes are called Cu(2). This definition can also be used for the 123 phase. Crystal structure of the 124 phase has been studied well by Wright and

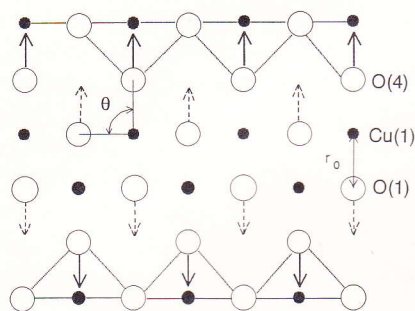


Fig. 1. Cross sectional view in b - c plane of the double Cu-O chain of the 124 phase. The interatomic distance between Cu(1) and O(1) is indicated by r_0 . Open circles indicate oxygen atoms and solid circles indicate copper atoms. O(1) A_g vibration mode is given by broken arrows and O(4) A_g mode by solid arrows. As frequency and amplitude of both vibrations are different, angle θ also vibrates.

Butler.¹⁸⁾ The nearest atom to Cu(1) in the 124 phase is oxygen atom called O(4) (Cu(1)–O(4) distance is 0.183 nm), and the next one is also oxygen atom called O(1) (Cu(1)–O(1) distance is 0.194 nm).¹⁸⁾ It has been reported that the doped silver atoms substitute with Cu(1) in the 123 phase. Assuming that silver atoms substitute also with Cu(1) in the 124 phase, the study of Cu(1)–O(4) and Cu(1)–O(1) vibrations will demonstrate an evidence to clarify whether silver atoms can replace copper atoms of the Cu(1) site in the 124 phase or not.

Raman spectra of the 123 phase have been well studied and most of the peaks are identified by Macfarlane et al.¹²⁾ and Yamanaka et al.¹³⁾ The Raman peak at about 500 cm⁻¹ corresponds to O(4)–Cu(1) stretching vibration in *c*-direction, and assigned as O(4)*A_g* mode.^{12),13)} Notice that the letter '*A_g*' indicates that the motion of O(4) atom is symmetrical for 360°/2 rotation with respect to *c*-axis, i.e., *C₂* rotation (letter *A*) and inversion (suffix *g*). It should be distinguished to the symbol of silver 'Ag'. Raman shift of O(4)*A_g* mode increases with increasing oxygen content.^{12),14)}

Raman spectra of the 124 phase have been studied by Heyen et al.^{15),16)} and all the peaks are identified and some of their results have been corrected by Yim et al.¹⁷⁾ Raman peak of the 124 phase at 605 cm⁻¹ corresponds to O(4)–Cu(1) stretching vibration in *c*-direction (called O(4)*A_g* mode), and that of 500 cm⁻¹ to O(1)–Cu(1) stretching vibration in *c*-direction (called O(1)*A_g* mode).¹⁷⁾ Solid arrows in Fig. 1 indicate O(4)*A_g* motion and broken arrows indicate O(1)*A_g* motion. In this work, both O(1)*A_g* and O(4)*A_g* vibrations of the 124 phase are studied as a function of silver content.

3. IR absorption spectra—the empirical scaling law

Lin et al. have proved a silver replacement into the Cu(1) site of the 123 phase by IR absorption method and the empirical scaling law for IR wave number, *k*, and interatomic distance, *d*, given by $kd^3 = \text{const.}$ for each atomic pair.⁹⁾

This law holds in C–N, C–O, P–S and Si–H systems.^{19),20)} An Ag–O bond with a length of 0.2043 nm in Ag₂O has a strong IR absorption peak at 540 cm⁻¹.²¹⁾ According to the $kd^3 = \text{const.}$ law, the constant is calculated as $kd^3 = 540 \times (0.2043)^3 = 4.6$.⁹⁾ Assuming that a silver atom enters into the Cu(1) site of the 123 phase, the interatomic distance between silver and oxygen can be estimated as 0.19 nm and the IR absorption wavenumber is calculated as $k = 670 \text{ cm}^{-1}$. Their IR absorption spectra showed that no absorption peak at $k = 693 \text{ cm}^{-1}$ was found for the silver free sample, but the peak appeared at $k = 693 \text{ cm}^{-1}$ and started to grow with increasing silver content. The wavenumber of this peak was in agreement with the calculated value (670 cm⁻¹) and they have concluded a silver replacement.⁹⁾ Similar

experimental evidence is discussed for the 124 phase in the present work.

4. Experimental procedure

Raw materials of 99.9% purity Y₂O₃, BaCO₃, CuO and AgO were mixed to prepare four different samples. The mixing ratio of the sample (i) is (Y : Ba : Cu : Ag) = (1 : 2 : 4 : 0) in atomic ratio, (ii) (1 : 2 : 3.96 : 0.04), (iii) (1 : 2 : 3.8 : 0.2) and (iv) (1 : 2 : 3.6 : 0.4), i.e., $x = \text{Ag}/(\text{Ag} + \text{Cu}) = 0, 0.01, 0.05$ and 0.1, in atomic fraction, respectively. All the samples were treated by an oxygen hot isostatic press (called O₂-HIP). O₂-HIP is a sintering equipment which can control temperature, *T*, total gas pressure, *P_{tot}*, as well as oxygen partial pressure, *P_{O₂}*, independently, and widely used to sinter oxides. Raw materials were formed into pellets, sintered at 1000°C under 200 MPa of *P_{tot}* and 40 MPa of *P_{O₂}* for 5h, and quenched by an adiabatic expansion of the surrounding atmosphere from *P_{tot}* = 200 MPa to 30 MPa in about 2 min. Cooling rate was about 12000 K · h⁻¹ (3 K · s⁻¹) from 1000 to 800°C, and 2000 K · h⁻¹ from 800°C to room temperature.²²⁾

IR absorption tests were carried out at room temperature on compressed pellets containing the ground samples (i)–(iv) mixed with KBr (with a weight ratio of samples; KBr = 1 : 100) in the range from 500 to 1000 cm⁻¹.

Raman scattering experiments were carried out at room temperature on sintered bodies in the range from 400 to 650 cm⁻¹. The excitation line of the 514.5 nm Ar⁺ at a power of 150 mW was used for calibration.

5. Results and discussion

Figure 2(a) shows Raman spectra of the AgO doped 124 phase. Figure 2(b) shows Raman shifts of O(4)*A_g* and O(1)*A_g* modes as a function of silver contents. Raman shift of O(1)*A_g* mode (at about 500 cm⁻¹) decreases, and that of O(4)*A_g* mode (at about 600 cm⁻¹) increases with increasing silver contents.

Raman shifts of O(1)*A_g* and O(4)*A_g* modes are calculated by GF matrix method.^{23)–25)} The GF matrix method gives the relationship between the force constants, atomic masses and Raman shifts. If λ is defined as $4\pi^2 c^2 k_R^2$, where *c* and *k_R* are light velocity and Raman shift, respectively, the approximate representation of λ for O(4)*A_g* mode is given by

$$\lambda = (f_1 + f_2) (\mu_O + \mu_{Cu}) \quad (1)$$

and

$$\lambda = \left(f_1 + \frac{\alpha_1}{r_0^2} \right) (\mu_O + \mu_{Cu}) \quad (2)$$

for O(1)*A_g* mode, where *f₁* is the O(4)–Cu(1) stretching force constant, *f₂* is the O(4)–Cu(2) stretching force constant and α_1 is the O(1)–Cu(1)–O(4) bending force constant. O(1)–Cu(1)–O(4)

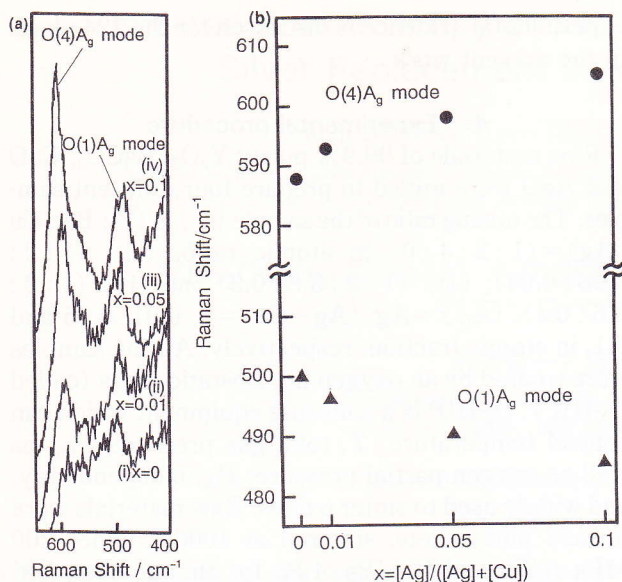


Fig. 2. (a) Raman spectra of the samples (i)–(iv). Raman shift of the O(1) A_g mode (about 500 cm^{-1}) decreases, and that of the O(4) A_g mode (about 600 cm^{-1}) increases with increasing silver content.

(b) Raman shifts of O(4) A_g and O(1) A_g modes as a function of silver content, x .

bending motion is the angular vibration of θ shown in Fig. 1. μ_{O} and μ_{Cu} are the reciprocal masses of oxygen and copper atoms, respectively. $r_0 = 0.183$ nm is the interatomic distance between Cu(1) and O(1) of the silver free sample.

Crystallographic data of the 124 phase are very similar to those of the 123 phase, thus we assumed the force constants of the 124 phase are same to those of the 123 phase. The values $f_1 = 160 \text{ N} \cdot \text{m}^{-1}$, $f_2 = 110 \text{ N} \cdot \text{m}^{-1}$ and $\alpha_1 = 1.3 \times 10^{-18} \text{ N} \cdot \text{mrad}^{-2}$ are used, as reported by Bates and Eldridge for the 123 phase.^{26,27} Then Raman shifts of the 124 phase are calculated as 594 cm^{-1} for O(4) A_g mode and 504 cm^{-1} for O(1) A_g mode, and they are in good agreement with the empirical values.^{15–17}

Figure 3 shows the X-ray diffraction patterns of the samples (i)–(iv). Solid circles indicate the 124 phase. Here we have to confirm the contribution to Raman peak at about 600 cm^{-1} from the 211 phase, because the 211 phase also has strong Raman scattering at about 600 cm^{-1} . Solid triangles in Fig. 3 indicate the 211 phase. Watanabe et al. has investigated that the addition of silver oxide favoured the formation of the 124 phase and the amount of impurity phases decrease with increasing silver content.⁷ It is also confirmed in our study that the amount of 211 phase decreases with increasing silver content. Raman peak at about 600 cm^{-1} grows and shifts toward high Raman shift with increasing silver content. There is no reason of growing and shifting of Raman scattering peak of the 211 phase with increasing silver content, and we can assume that the Raman peak at about 600 cm^{-1} is that of O(4) A_g mode in 124 phase. In Fig. 3, small peaks of metallic silver also can be seen at about 38 and 44 degrees of diffraction

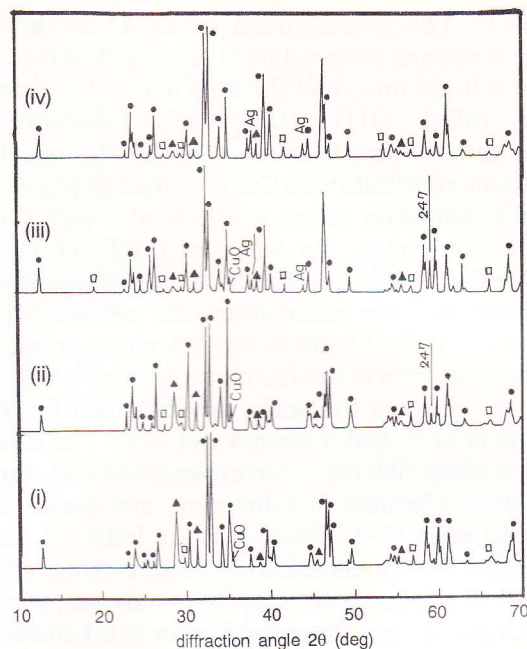


Fig. 3. X-ray diffraction patterns of the samples (i)–(iv). Solid circles indicate 124 phase, solid triangles 211 phase. Metallic silver appears in (iii) and (iv). Open squares indicate the peaks we could not investigate.

angle in the samples of $x = 0.05$ and 0.1. It seems that the silver solubility limit is a value between $x = 0.01$ and 0.05. Open squares indicate the peaks we could not investigate.

Raman shift of O(4) A_g mode increases, and that of O(1) A_g mode decreases with increasing silver content as shown in Fig. 2(b). Raman shifts of O(4) A_g and O(1) A_g modes are given by Eqs. (1) and (2), respectively, and the experimental results suggest that the force constant f_1 decreases and f_2 increases by doping silver. A phenomenological calculation is shown as follows.

Force constant can be estimated from bonding energy, interatomic distance and the potential formula. Interatomic distances and bonding energies of Cu(1)–O(4), Cu(2)–O(4) and Ag(1)–O(4) are necessary. Cu–O bonding energy of Cu_2O is about 930 eV and interatomic distance is about 0.184 nm, and Ag–O bonding energy of Ag_2O is about 370 eV and interatomic distance is about 0.205 nm.²⁸ Cu(1)–O(4) distance is 0.183 nm and Cu(2)–O(4) distance is 0.229 nm,¹⁸ and we assume that Cu(1)–O(4) bonding energy is 930 eV and Ag(1)–O(4) bonding energy is 370 eV.

Wright and Butler have reported that the potential formula of O(4) atom with respect to Cu(1) in the 123 phase can be written as $U(r) = Ar^{-8} - Br^{-1}$, where r is interatomic distance.¹⁸ Constants A and B can be calculated by the condition $U(r_0) = \text{bonding energy}$ and $(dU/dr)_{r_0} = 0$, where r_0 is the interatomic distance at 0 K. Force constant can be estimated by calculating the second derivative of $U(r)$ with respect to r , i.e., $-(d^2U/dr^2)_{r_0}$. If the value of r_0 (Ag(1)–O(4)) is equated to 0.205 nm and 370 eV of bonding energy, the force constant between Ag(1)

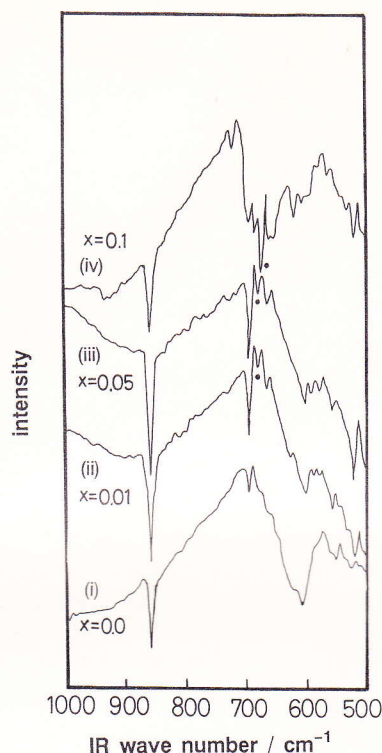


Fig. 4. IR absorption spectra of the samples (i)–(iv). Silver doping quantity x indicates as an atomic fraction $\text{Ag}/(\text{Cu} + \text{Ag})$. The absorption peak at $k=675 \text{ cm}^{-1}$ (solid circles), which indicates Ag–O bonding, grows with increasing x .

and $\text{O}(4)$, f_1' , can be estimated as about $50 \text{ N} \cdot \text{m}^{-1}$. In the same way, $r_0(\text{Cu}(2)\text{--O}(4))$ is equated to 0.2 nm and force constant after silver replacement, f_2' , can also be estimated as about $130 \text{ N} \cdot \text{m}^{-1}$. These simple calculations show that f_1 decreases and f_2 increases by doping silver. But these simple calculations conclude that Raman shifts of both of $\text{O}(4)A_g$ and $\text{O}(1)A_g$ modes decrease. It should be shown by the thorough calculation that both force constants f_1' and f_2' have same value about $150 \text{ N} \cdot \text{m}^{-1}$, and in this case Raman shift of $\text{O}(4)A_g$ mode increases while that of $\text{O}(1)A_g$ mode decreases. Thus Fig. 2 indicates that the doped silver substitutes into $\text{Cu}(1)$ site in the 124 phase.

Figure 4 shows the IR absorption spectra of the AgO doped 124 phase in the range of $500\text{--}1000 \text{ cm}^{-1}$ wavenumber. Absorption peaks at $k=700$ and 880 cm^{-1} indicate BaCO_3 . The interatomic distance between $\text{Cu}(1)$ and $\text{O}(4)$ in the 124 phase is almost same as that of the 123 phase,¹⁸⁾ and the IR absorption peak should appear at the same position (about 670 cm^{-1}). The absorption peak at $k=675 \text{ cm}^{-1}$ increases with increasing silver content up to $x=0.1$. This peak is not the peak of AgO (AgO peaks appear at $k=550$ and 705 cm^{-1}). According to Lin's theory,⁹⁾ Fig. 4 suggests that a silver atom substitutes into the $\text{Cu}(1)$ site in the 124 phase.

6. Conclusion

$\text{YBa}_2(\text{Cu}_{1-x}\text{Ag}_x)_4\text{O}_8$ superconductors are synthesized by oxygen hot isostatic press. Silver replace-

ment into $\text{Cu}(1)$ site is confirmed by Raman scattering method and IR absorption method.

Acknowledgements The authors would like to express their gratitude to "Monbusho" (Ministry of Education and Culture) as well as to Kobe Steel Co., Ltd. (Kobelco) for providing an excellent support to the present work through the Cooperative Program.

References

- 1) B. Dwir, M. Affronte and D. Pavuna, *Physica C*, **162**, 351–55 (1989).
- 2) N. Imanaka, F. Saito, H. Imai and G. Adachi, *J. J. Appl. Phys.*, **284**, L580–82 (1989).
- 3) G. Kozłowski, S. Rele, D. F. Lee and K. Salama, *J. Mater. Sci.*, **26**, 1056–60 (1991).
- 4) Y. Ren, J. Meng, M. Niu and Z. Zeng, *Solid State Commun.*, **76**, 1103–05 (1990).
- 5) Y. Sawai, K. Ishizaki, M. Takata and Y. Narukawa, *Solid State Phenomena*, **25**, 26, 363–70 (1992).
- 6) B. Souletie, M. Guillot, P. Lejay and J. L. Tholence, *Solid State Commun.*, **78**, 717–21 (1991).
- 7) Y. Watanabe, K. Yanagida, M. Takata and K. Ishizaki, *Physica C*, **190**, 84–86 (1991).
- 8) K. K. Singh, P. D. Hunneyball and P. P. Edwards, *J. J. Appl. Phys.*, **30**, 3364–70 (1991).
- 9) J. J. Lin, T. M. Chen and Y. F. Chen, *Solid State Commun.*, **76**, 1285–90 (1990).
- 10) B. A. Kolesov, N. F. Zakharchuk, I. G. Vasilyeva, L. I. Yundanova, L. P. Kozeeva, S. A. Gromilov and M. A. Starikov, *Solid State Commun.*, **84**, 645–49 (1992).
- 11) J. H. Choy, D. Y. Jung, J. C. Grenier, J. C. Park and A. Wattiaux, *Materials Letters*, **10**, 121–25 (1990).
- 12) R. M. Macfarlane, H. J. Rosen, E. M. Engler, R. D. Jacowitz and V. Y. Lee, *Phys. Rev. B*, **38**, 284–89 (1988).
- 13) A. Yamanaka, F. Minami, K. Watanabe, K. Inoue, S. Takekawa and N. Iyi, *J. J. Appl. Phys.*, **26**, L1404–06 (1987).
- 14) C. Thomsen, R. Liu, M. Bauer, A. Wittlin, L. Genzel, M. Cardona, E. Schonherr, W. Bauhofer and W. König, *Solid State Commun.*, **65**, 55–58 (1988).
- 15) E. T. Heyen, M. Cardona, J. Karpinski, E. Kaldis and S. Rusiecki, *Phys. Rev. B*, **43**, 12958–75 (1991).
- 16) E. T. Heyen, R. Liu, C. Thomsen, R. Kremer, M. Cardona, J. Karpinski, E. Kaldis and S. Rusiecki, *Phys. Rev. B*, **41**, 11058–67 (1990).
- 17) K. K. Yim, J. Oitmaa and M. M. Elcombe, *Solid State Commun.*, **77**, 385–88 (1991).
- 18) N. F. Wright and W. H. Butler, *Phys. Rev. B*, **42**, 4219–27 (1990).
- 19) G. Lucovsky, *Solid State Commun.*, **29**, 571–76 (1979).
- 20) A. L. Smith and N. C. Angelotti, *Spectrochim. Acta*, **14**, 412–20 (1959).
- 21) N. T. McDevitt and W. L. Baun, *Spectrochim. Acta*, **20**, 799–800 (1964).
- 22) Y. Sawai, K. Ishizaki, M. Takata and Y. Narukawa, *Physica C*, **176**, 147–50 (1991).
- 23) S. Mizushima and T. Shimanouchi, "Infrared Absorption and Raman Effects", Kyoritsu Co., Japan (1976) pp. 116–46.
- 24) K. Nakamoto, "Infrared and Raman Spectra of Inorganic and Coordination Compounds, Fourth ed.", Wiley-Interscience Publication, New York (1986) pp. 18–63.
- 25) T. Shimanouchi, M. Tsuboi and T. Miyazawa, *J. Chem. Phys.*, **35**, 1597–612 (1961).
- 26) F. E. Bates, *Phys. Rev. B*, **39**, 322–27 (1989).
- 27) F. E. Bates and J. E. Eldridge, *Solid State Commun.*, **64**, 1435–39 (1987).
- 28) M. Romand, M. Roubin and J. P. Deloume, *J. Electron Spec. Related Phenom.*, **13**, 229–42 (1978).
- 29) G. F. Voronin and S. A. Degterov, *Physica C*, **176**, 387–408 (1991).